Int. J. Appl. Math. Comput. Sci., 2022, Vol. 32, No. 1, 111–123
DOI: 10.34768/amcs-2022-0009

PERFORMANCE ANALYSIS OF A DUAL STAGE DEEP RAIN STREAK REMOVAL CONVOLUTION NEURAL NETWORK MODULE WITH A MODIFIED DEEP RESIDUAL DENSE NETWORK

THIYAGARAJAN JAYARAMAN [a,*], GOWRI SHANKAR CHINNUSAMY [b]

[a]Department of Mechatronics Engineering
Sona College of Technology
Junction Main Road, Salem, Tamil Nadu, India
e-mail: jthiyagarajanphd20@gmail.com

[b]Department of Electrical and Electronics Engineering
KSR College of Engineering
KSR Kalvi Nagar, Namakkal, Tamil Nadu, Tiruchengode, India
e-mail: cgsshankarme@gmail.com

The visual appearance of outdoor captured images is affected by various weather conditions, such as rain patterns, haze, fog and snow. The rain pattern creates more degradation in the visual quality of the image due to its physical structure compared with other weather conditions. Also, the rain pattern affects both foreground and background image information. The removal of rain patterns from a single image is a critical process, and more attention is given to remove the structural rain pattern from real-time rain images. In this paper, we analyze the single image deraining problem and present a solution using the dual stage deep rain streak removal convolutional neural network. The proposed single image deraining framework primarily consists of three main blocks: a derain streaks removal CNN (derain SRCNN), a modified residual dense block (MRDB), and a six-stage scale feature aggregation module (3SFAM). The ablation study is conducted to evaluate the performance of various modules available in the proposed deraining network. The robustness of the proposed deraining network is evaluated over the popular synthetic and real-time data sets using four performance metrics such as the peak signal-to-noise ratio (PSNR), the feature similarity index (FSIM), the structural similarity index measure (SSIM), and the universal image quality index (UIQI). The experimental results show that the proposed framework outperforms both synthetic and real-time images compared with other state-of-the-art single image deraining approaches. In addition, the proposed network takes less running and training time.

Keywords: single image deraining, deep learning, modified residual dense network, PyTorch.

1. Introduction

Rainy weather conditions greatly affect the visibility of scene objects in captured real-time images. Also, the visual quality of a real-time high-definition image is mainly affected under outdoor weather conditions such as rain, snow and fog. The poor visual quality significantly affects the nature of computer vision, image surveillance, and multimedia applications. Therefore, removing the rain pattern from the high-definition images is an important pre-processing step in real-time multimedia applications (Ding *et al*., 2016; Barnum *et al*., 2009). The rainy image is expressed as the linear sum of a background image and a rain layer. Restoration of an affected image by rain streaks is a critical problem due to numerous interconnection possibilities between the rain and background layers (Garg and Nayar, 2004). Many deraining priors about the separation of the background image and the rain layer are proposed by Kim *et al*. (2013). These prior-based deraining methods fail to provide superior performance when images are affected by different shapes and orientations of rain patterns (Kang *et al*., 2012; Kou *et al*., 2015).

Fu *et al*. (2017) proposed a derain net framework to remove rain streaks from a single image. In this

*Corresponding author

framework, a deep convolutional neural network (DCNN) is used to map the relationship between rainy and clean images. A bilateral recurrent network (BRN) is proposed by Ren *et al*. (2020) to remove the rain pattern from a single image synthetic data set. This network combines the advantages of a single recurrent network and bilateral long short-term memory (LSTMs) based draining approaches. The performance of the BRN deraining concept is proved on various image data sets for three stages only. The number of deraining stages increases beyond three; this network yields a larger training error. An optimized multi delay block frequency domain (OMBFD) adaptive filter is proposed by Thiyagarajan and Gowri Shankar (2020) to remove the low-intensity rain pattern. In this adaptive filter, the firefly optimization algorithm involves additional deraining complexity. The adaptive filter-based deraining frameworks are only suitable to handle low-intensity rain patterns.

Wang *et al.* (2020a) proposed a spatial contextual information aggregation module and a pyramid network module for deraining applications. A spatial contextual information aggregation module is used to acquire the multi-scale features from the kernels of the rainy image. The pyramid network module is utilized to connect the features of rain streaks. The dilation factor of this network is one of the limiting factors to achieve better deraining results. Wang *et al*. (2019) proposed a rain removal framework based on the gradient magnitude and directions of rain patterns. In the high-frequency domain, the rain component is identified and removed. But this method eliminates some of the fine components of the original image. The contextual information is very important to remove the rain pattern due to the availability of rain patterns with different sizes and shapes. This information is extracted by the recursive modified dense network through batch normalization layers (Chen and Wang, 2020). The network depth increases automatically, which affects the complexity of the deraining process.

In recent days more and more deep-learning-based end-to-end deraining models have been being proposed to remove the rain pattern. But they fail to provide satisfactory results in different realistic conditions like heavy rain streaks haze accumulated effect of rain patterns (Wang *et al.* 2020b, 2020d). An enhanced video block matching four-dimensional (V-BM4D) deraining framework is proposed by Jayaraman and Chinnusamy (2020b) to remove the structural rain pattern from the successive video frames. Hence the rain pattern is predicted in the 4D domain. This filtering concepts provides nominal visual quality improvements for single image deraining applications (Koziarski and Cyganek, 2018). A mathematical linear model of the rain image is developed to analyze the rain pixel correlation with the original image (Wang *et al.*, 2020c). The cost function plays an important role in removing rain patterns from the background. This linear model is evaluated until a low-cost function is achieved. In this method, some of the non-rain details which have similar intensity are misguided as rain pattern. A nonlinear mapping study has been developed through MSFA-Net for both rainy image and clean image data sets (Wu and Zhou, 2020; Papiez *et al*., 2019). This method is more time-consuming for heavy rain streaks. Li *et al*. (2020) designed a novel channel attention U-dense network for rain pixel detection and a residual dense block for rain streak removal. The U-dense network is used to achieve pixelwise estimation accuracy and rain features are exploited by a dense block. Experimental results demonstrate that this model-based deraining method offers the minimum level of PSNR improvement compared with state-of-the art methods.

A deep rain streak removal CNN (DeRain SRCNN)-based deraining framework is proposed with two residual block layers and a dual channel rectification linear unit (DCReLU) (Jayaraman and Chinnusamy, 2020a; Kowal *et al*., 2021). This deraining network provides higher PSNR and SSIM values for both synthetic and real-time images compared with other existing deraining networks. The convergence policy of this network is more suitable for deraining applications. But this network faces some training errors and poor image visual quality for images with high rain patterns. The comprehensive loss function optimization and recovering original information are the two important steps in any deraining network. Sharma *et al*. (2021) proposed high-resolution image deraining using conditional generative adversarial networks (HRID-GAN) to achieve fewer artifacts and good visual quality. Image deraining can be categorized based on (i) supervised models with labeled constraints, (ii) semi-supervision based learning paradigms, and (iii) unsupervised models with self-supervised constraints. However, a majority of the state-of-the-art deraining methods adopt supervised learning with labeled-constrained models, trained on synthetically generated data sets.

The novelty and main contribution of this paper are as follows:

(i) A dual stage derain SRCNN module is proposed to solve the deraining problem. The reconstructed image from the derain SRCNN block and the original rain image act as input for the modified dense network block to further locate rain components in the output of the first stage derain SRCNN block.

(ii) A modified residual dense block (MRDB) is proposed to model and learn the rain components. A six-stage scale feature aggregation module (3SFAM) is introduced to transform the different scales of the derained image into the final output image.

(iii) The cascading of the MRDB and 3SFAM block offers the image rain components extraction, refinement and transformation.

(iv) A dual channel rectified linear unit is used as an activation function in the derain SRCNN block and the modified dense network block to resolve the network gradient issues.

The rest of this paper is organized as follows. Section 2 presents the architecture of the proposed dual stage derain SRCNN module with a deep residual dense network. The performance evaluation through experiments results is presented in Section 3. Finally, Section 4 concludes this paper.

2. Proposed deraining framework

This section briefly introduces the proposed single image deraining framework based on residual dense networks. This deraining framework consists of modules such as the two-stage derain streak removal CNN module, the modified residual dense block and the six-stage scale feature aggregation unit. The derain SRCNN module is mainly used to predict the rain components and act as the core module of this proposed deraining module. The rain pattern modeling and elimination are performed using the modified residual dense block. In this MRDB module, the DeReLU activation function is used to detect various statistically independent rain patterns. Rain image features in different scales are aggregated using the six-stage scale aggregation module.

The deep-learning-based single image deraining method provides an effective learning policy to identify the rain patterns from the original images. Also, it offers a very smooth linear relation between the foreground information and the background image information. Due to the behavior of the deep network, it is easy to separate the rain components from background details. Moreover, the background information retention accuracy is more in the deep-learning-based deraining approach. Since the rain patterns have different sizes and orientations, the correlation between the rain pattern and the background is notably observed through training stages of deep networks.

The general topology of the proposed rain streak removal framework is shown in Fig. 1. This network is designed with two distinct stages to handle the rain component distributions. The rainy image denoted as R is fed into the two-stage derain SRCNN block and generates the first derain image (DR1). The derain image (DR1) and the rain image (R) are then concatenated to form a tensor image, which is given to the modified dense network block. This second stage deraining process generates the reconstructed image denoted as the second derain image (DR2). Hence DR2 contains some rain components in the background scene, so that DR2 is compared with the original rain image R. The convolutional layer and DcReLu are used to get the visually improved image DR3.

The proposed derain framework is mainly composed of a cascade of different distinct modules including the derain SRCNN, MRDB, and 3SFAM. The synchronous tuning of the two-stage module block plays an important role in this deraining process. The contribution of all modules is described as follows. The derain SRCNN block consists of a two-stage module. An internal structure of Stage I is shown in Fig. 2. This stage is a single derain streak removal CNN block which contains the parallel residual inception module, the middle layer module, the batch normalization (BN) unit, and the output inception module. The rain streak affected image is passed through a stack of the convolutional layer and the downsampled pooling layer to identify the rain components. The parallel residual inception module is constructed using two residual blocks connected in parallel and the global averaging pooling layer. This first inception module of the derain SRCNN is used to extract the low-level and high-level features from the input rain image. The residual block is constructed using two convolutional layers with 3×3 kernel size and a dual channel ReLU (DCReLU) activation function. The DCReLU activation function improves the training time speed compared other activation functions.

The intermediate module consists of an additional convolutional layer with a 2×2 filter size. The rain streaks are more directional oriented so that more convolutional layers with filter size 3×3 are used along with the pooling layer. A batch normalization module is introduced between the intermediate module and the output module to avoid vanishing gradient issues and poor learning capacity. This BN module contains a convolutional layer with 5×5 kernel size and a pooling layer with a stride value of 2. The final inception module is used to concatenate all the selected feature maps to obtain a reconstructed image

2.1. Modified residual dense block. The dense net transmits the extracted feature in each layer of the network to obtain a visually enhanced result. The modified residual dense block is designed to extract main features from the input rainy images. The basic dense block is constructed using the ReLU activation function. A poor convergence rate is achieved using a basic residual dense block. Therefore, a dual channel ReLU is adopted in the modified residual dense block to achieve a better convergence time of the proposed deraining network. Figure 3 shows the building blocks of the MRDB module. This dense block is developed from the ResNet (He *et al.*, 2016), DenseNet (Huang *et al.*, 2017), and the Residual Dense Block (Zhang *et al.*, 2018). The convolutional layer with a 3×3 filter is used along with the DcReLu activation

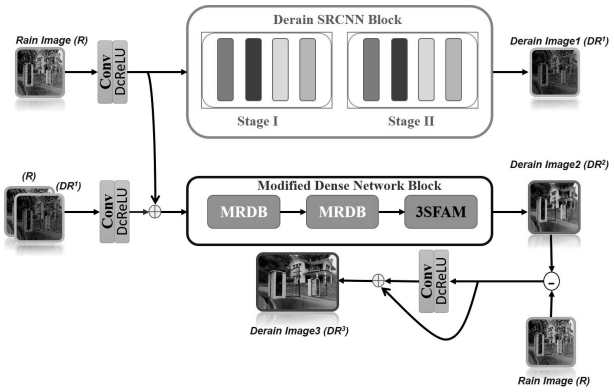

Fig. 1. Overall architecture of the proposed dual stage derain SRCNN module with a deep residual dense network.

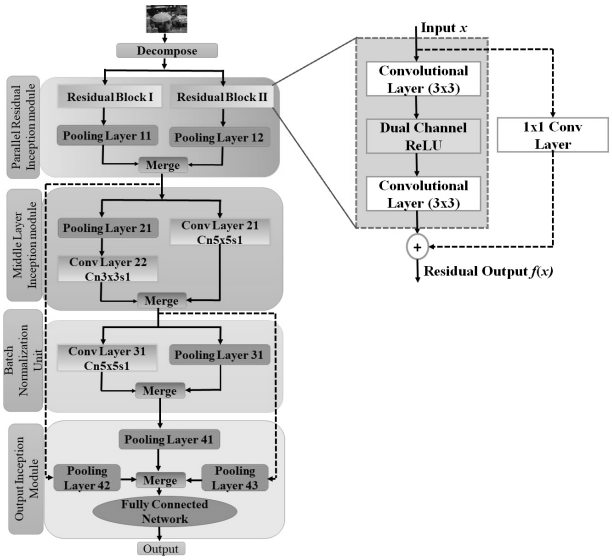

Fig. 2. Internal structure of the derain streak removal convolutional neural network (derain SRCNN).

function to extract the rain features. A dual-channel ReLU is used as an activation unit in the modified RDB units. The usage of DcReLU in this residual block helps to mitigate the gradient instability during the training stages of the proposed deraining network. The DcReLU activation function identifies the features in both positive and negative phases of image sequences compared with the ReLU activation function. The gradient instability is also mitigated by feature reuse in this dense block. From the detailed experimentation presented in this work, it is observed that the MRDB unit identifies the finer rain features as well as achieves a better convergence rate.

2.2. Six-stage scale feature aggregation module. Transformation of the feature map domain into an image domain is an important process in deraining applications. The six-stage scale feature aggregation module shown in Fig. 4 is designed to map the feature domain into the output image space. This six-stage aggregation module captures all fine features and converts them into to the image domain. In most deep learning-based deraining algorithms, only a convolution layer is used to map the feature map with the output image domain. But the convolutional layer fails to capture the rich features on a different scale from the feature map.

The structural rain pattern penetrates through the entire image plane. Consequently, it is necessary to analyze the rain image on a different scale. The dual-stage deraining networks consist of a six-stage scale feature aggregation module to capture the fine original details and maintain the visual quality of the image. Six stages are sufficient to extract fine features from the modified dense network block. The number of stages increased beyond six; it is observed that the same visual quality is achieved. But the computational complexity and

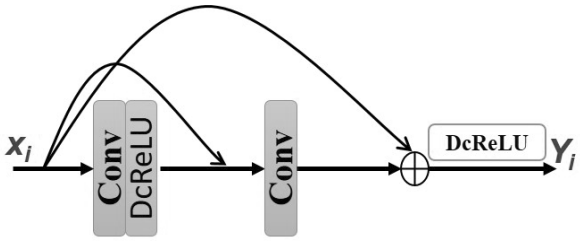

Fig. 3. Building block of the modified residual dense block (MRDB).

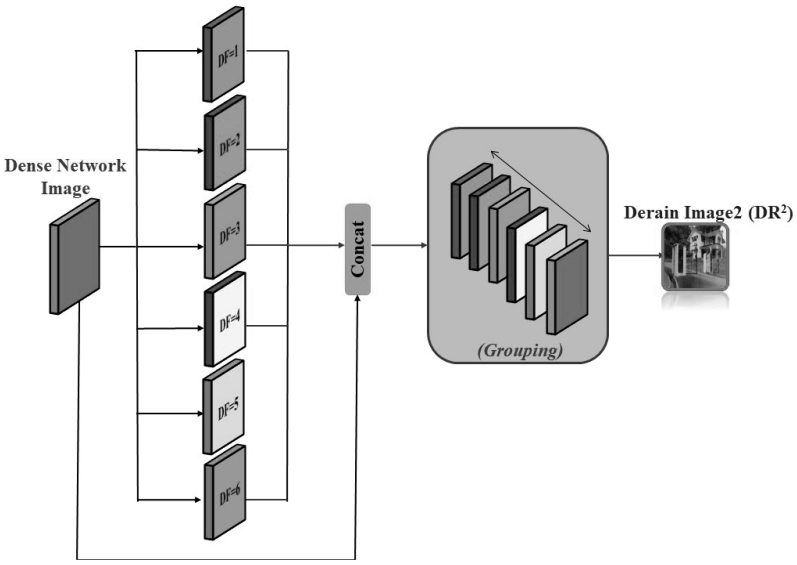

Fig. 4. Six-stage scale feature aggregation module.

convergence time of the proposed network increases up to 25%. Hence, it affects the implementation policy of the proposed deraining network. In this 3SFAM, six dilated convolution layers with a kernel size of 3×3 are used to identify the fine rain features. The feature map produced by six dilated layers is concatenated to get the final output rain-free image.

2.3. Loss function. For a single image deraining application, the regression loss function is sufficient to calculate the error between the derained output and the rain image. The regression mean-squared error loss function is

$$L(x) = \frac{1}{2}\|Y_{\text{in}} - Y_{\text{est}}\|^2 \tag{1}$$

where Y_{in} is the input rain image and Y_{est} is the estimate of the reconstructed image. The gradient of the loss function provides the direction in which the cost function has a steepest rate of increase. The stochastic gradient algorithm (SGD) takes more time to converge for the deep neural network in deraining applications. The SGD with a gradient clip optimization system is employed in the proposed deraining network to avoid the convergence explosion problem. The SGD weights are updated as

$$W^{k+1} = W^k - \eta \Delta L(x), \tag{2}$$

where η defines the learning rate of the network and $\Delta L(x)$ defines the gradient of the loss function. The training of the network becomes unstable when there are more feature maps.

The learning rate η is a basic hyperparameter used to train the CNN. It is a small positive value between 0.0 and 0.1. By taking a small value of the initial learning rate, the network requires more training epochs to converge and a larger value of the learning rate yields rapid convergence of the network with fewer training epochs. The selection of the initial learning rate is a challenging task in the deep neural network. In our proposed dual-stage derain SRCNN framework, the SGD optimization algorithm with the exponential decay learning rate scheduling method is used to achieve better network model accuracy. The exponential decay learning rate mechanism provides the required validation accuracy of the proposed network compared with other learning rate strategies such as the time-based decay and step decay methods. The initial learning rate is 0.001 for the first 50 epochs and then

the learning rate is reduced gradually for the remaining epochs. Network training is improved by the momentum factor.

3. Experimental results and a discussion

In this section performance analysis of the proposed network is presented. For performance experiments, we have considered popular synthetic rain data sets including joint convolutional analysis and synthesis (JCAS) (Gu *et al*., 2017), the recurrent squeeze and excitation context aggregation network (RESCAN net) (Li *et al*., 2018), the deep derail network (DDN net) database (Fu *et al*., 2017), the density aware single image deraining multistream dense network (DID MDN net) (Zhang and Patel, 2018), Rain12 (Li *et al*., 2016), Rain100L and Rain100H (Yang *et al*., 2017). The JORDER network provides Rain100H and Rain100L, each of which consists of 100 ground truth and rain images. This network consists of low-resolution and high-resolution rain images for predictions. The derain SRCNN provides 200 image pairs with different orientations. This data set consists of low-intensity rain images, medium rain images, and heavy rain streak-affected images. The DID MDN provides 350 synthetic clean images and rain images for training the deraining networks.

The testing and training of the deraining networks is conducted on a PC with Intel i5 CPU, 16GB RAM, and NVIDIA Geforce GTX 2070. The PyTorch (Paszke *et al*., 2019) open-source framework is used to train both synthetic and real-world single rain images. Since PyTorch is an open-source deep-learning library for Python, it is useful for applications such as natural language processing video processing. PyTorch provides tensor computation with strong GPU acceleration compared with other open-source tools. The tensor in PyTorch is similar to the NumPy array. Additionally, this tensor can be used on a GPU. The main elements of PyTorch are PyTorch tensors, operations, the autograd module, the optimization module, and the NN module. PyTorch provides more than 200 mathematical operation interfaces. Pytorch and Tensorflow are popular open-source package used for deep learning applications. The PyTorch platform provides the Scalable distributed training and testing for CNN-based deraining frameworks. Also, PyTorch offers good performance optimization in both CPU and GPU platforms.

3.1. Hyperparameter selection. The selection of the hyperparameters (the learning rate, the batch size, the momentum, and the weight decay) for the CNN is performed on a trial-and-error basis. The hyperparameters play an important role in training the deraining model. The optimal value of these hyperparameters provides better convergence results of the proposed network. The learning rate helps to regularize the training of the proposed deraining network. The selection of the learning rate is very important for this dual-stage deraining network. In this work, we have considered the learning rate between 10^{-5} and 10^{-1}. Within these limits, the proposed network offers a better convergence time. For the training scenario, the proposed network is tested with a learning rate of 10^{-3}. By considering a higher value of the learning rate, network overfitting is avoided. The momentum and learning rates are interrelated. Higher momentum values are mostly used to avoid network instability during the training and testing phases.

In this proposed method, we have tried to test the deraining framework with two momentum values such as 0.95 and 0.97. A higher value of momentum (0.97) is considered for training the dual-stage deraining module. Also, we observed that earlier convergence of the proposed network happens when the momentum value is 0.97. The batch size also affects the computational time of the deraining network. Since the proposed method is tested with a higher-end hardware platform, a higher batch size is suitable for training the deraining module. The complete performance analysis of the dual-stage deraining framework is done with a batch size of 32. The computational time of the deraining network is reduced by 27% compared with a batch size of 16.

The deraining performance of the proposed network is also extended for real world rain data sets including the spatial attentive network (SPA net) database (Wang *et al*., 2019), joint rain detection and removal JORDER-E (Yang *et al*., 2020), the semi-supervised image rain removal database (SSIR) (Wei *et al*., 2018), the progressive image deraining network (PReNet) (Ren *et al*., 2019). The validation of the proposed deraining network is based on a training set, a validation set, and a training set. In this work, we have considered both synthetic and real-time rainy images for analysis purposes. The data set dividing policy plays an important role in validating the proposed method. From each of the data sets, 80% of total image samples are considered for the training phase. The remaining image samples are considered for validation purposes. The SGD with gradient clip optimization technique is employed in this deraining method with a mini-batch size of 32. The network was trained using 250 epochs to achieve the required convergence and attain a higher deraining process. From the performance investigation, it is observed that the network attains convergence below 100 epochs for the synthetic data set. For the real-time data set, the proposed deraining network takes 150 to 170 epochs based on types of rain structures. The hyperparameters are selected through cross-validation of the different rainy data sets.

3.2. Performance measures. The effectiveness of the proposed method is demonstrated by conducting

Table 1. Performance metric comparison of state-of-the arts methods and the proposed method on a synthetic data set.

Data set	Metric	Rain frame	JORDER	SSDRNET	Proposed
RAIN100L	PSNR	33.25	34.15	36.77	40.12
	SSIM	0.9525	0.9611	0.9689	0.9748
	FSIM	0.9632	0.971	0.9792	0.9862
	UIQI	0.8478	0.8591	0.8644	0.9015
RAIN100H	PSNR	27.12	28.87	31.28	35.79
	SSIM	0.8726	0.8811	0.9145	0.9511
	FSIM	0.9265	0.9315	0.9488	0.9815
	UIQI	0.7954	0.8114	0.8377	0.8815
DID MDN	PSNR	30.38	32.85	36.25	40.75
	SSIM	0.8377	0.8415	0.8764	0.9015
	FSIM	0.9378	0.9465	0.9633	0.9891
	UIQI	0.8611	0.8713	0.8878	0.9122
DDN net	PSNR	35.81	36.62	38.15	42.17
	SSIM	0.9322	0.9417	0.9676	0.9912
	FSIM	0.9478	0.9565	0.9721	0.9902
	UIQI	0.8725	0.8814	0.8966	0.9117
RESCAN net	PSNR	25.12	27.33	29.55	34.72
	SSIM	0.8825	0.8915	0.9025	0.9244
	FSIM	0.9155	0.9211	0.9286	0.9468
	UIQI	0.7564	0.7745	0.7915	0.8244

more numerical experiments on a different synthetic data set and real-world data sets. The performance of the proposed deraining experiments is evaluated using different reference quality metrics (Wang *et al*., 2004). The peak signal-to-noise ratio (PSNR) (Sheikh and Bovik, 2006), the structural similarity index (SSIM) (Wang *et al*., 2004), the feature similarity index (FSIM) (Zhang *et al*., 2011) and the universal image quality index (UIQI) (Wang and Bovik, 2002) are used as performance metrics in this work. The FSIM metric is mainly used to predict the amount of the rain feature available in the reconstructed image. The performance of the proposed dual stage derain SRCNN module with the deep residual dense network is compared with two deep learning-based deraining methods such as rain detection and removal JORDER (Yang *et al*., 2017) and the sequential dual attention network-based single image deraining deep network SSDRNET (Lin *et al*., 2020). In this research analysis, four performance metrics are calculated for various synthetic rain data sets including Rain100L, Rain100H, DID MDN, the DDN net and RESCAN. All the five synthetic rain data sets are involved in the training and testing processes. The values of the corresponding performance metrics are presented in Table 1.

UIQI (universal image quality index) is a kind of the structural similarity index (SSIM). This index is also used to capture the fine intensity similarity of two images. Hence, the rain pattern shows the different structures in the entire image location. The UIQI is the best option to measure the fine rain pattern similarity between the original image and the derained image. In this work, both FSIM and UIQI similarity measures are more useful to prove the effectiveness of the proposed dual-stage deep rain streak removal CNN-based deraining framework. The achieved values of these two similarity measures is shown in Tables 1 and 2. From Table 1, it is observed that the proposed deraining framework offers higher PSNR and SSIM values compared with other existing methods. so that the proposed dual-stage derain SRCNN-based attention network performs on any kind of rain pattern. The dual-stage derain SRCNN deraining policy offers a 3.56 dB PSNR improvement for Rain100L and Rain100H data sets compared with other approaches.

Overall, applying the rain streaks affected synthetic data set to the proposed dual state derain SRCNN deraining frameworks, it is observed that the PSNR value increases from 3 dB to 12.5 dB and from 3% to 22% for the SSIM value improvement observed in reconstructed derained images. From the various numerical performance experiments, the proposed method eliminates any kind of rain pattern from the original image without degrading the visual quality.

The deraining performance of the proposed network is also tested for different real-world image data sets including JORDER-E, SSIR, PReNet, Rain Heavy, and the SPA net. More numerical training and testing experiments are conducted on real-world image data sets. The corresponding performance metric values are presented in Table 2.

For real-world image data sets, the proposed

Table 2. Performance metric comparison of state-of-the arts methods and the proposed method on a real data set.

Data set	Metric	Rain frame	JORDER	SSDRNET	Proposed
JORDER-E	PSNR	24.16	27.33	29.15	33.54
	SSIM	0.8145	0.8246	0.8344	0.8612
	FSIM	0.7586	0.7712	0.7856	0.8125
	UIQI	0.7126	0.7315	0.7425	0.7561
SSIR	PSNR	37.12	38.77	39.6	42.59
	SSIM	0.8516	0.8601	0.8745	0.9011
	FSIM	0.9365	0.9415	0.9518	0.9795
	UIQI	0.7054	0.7114	0.7265	0.7552
PRENET	PSNR	33.38	34.85	36.15	40.15
	SSIM	0.8177	0.8315	0.8404	0.8615
	FSIM	0.8378	0.8465	0.8633	0.8891
	UQI	0.7611	0.7745	0.7798	0.7922
Rain Heavy	PSNR	37.01	38.62	39.75	43.57
	SSIM	0.9422	0.9457	0.9696	0.9812
	FSIM	0.9178	0.9255	0.9321	0.9512
	UQI	0.8125	0.8244	0.8322	0.8485
SPANET	PSNR	29.34	31.24	33.22	35.45
	SSIM	0.8452	0.85	0.8599	0.8689
	FSIM	0.9125	0.9255	0.931	0.9422
	UQI	0.8215	0.8311	0.8422	0.8615

deraining approach offers 2 dB to 9.5 dB of the PSNR value improvement and 5% to 15% of the SSIM value improvement. Also, the visual quality of the reconstructed image is assessed using feature reference metrics FSIM and UIQI. The FSIM metric value gives the information about rain elimination accuracy. UIQI is used to assess the background degradation due to rain patterns. From Tables 1 and 2 it is observed that the proposed method provides higher FSIM and UIQI values on the synthetic data set and real-world data sets.

Figure 5 shows the deraining results of various deraining networks on a synthetic data set. The first and second rows show the deraining results Rain100L and Rain 100H data set, respectively. Observing the results obtained from the proposed method, rain patterns are completely removed and the visual quality is also improved. Observing Fig. 5, the JORDER net and SSDRNET remove only part of the rain pattern from the image. But the proposed dual-stage derain SRCNN-based attention network removes the direction-oriented rain pattern completely compared with ground truth image sequences. For the synthetic image data set, the proposed method removes the small and large rain streaks completely from the corrupted background.

Figure 6 shows the deraining performance results on a real-world data set. The first row shows the deraining results of the sportsman ground truth image. From this result, it is observed that rain images containing different intensity background information and the rain information are mixed with various levels of background information. The background details are affected due to the usage of the JORDER net and SSDRNET methods. The proposed method removes the rain pixel as much as possible while preserving the background information. The third row of Fig. 6 shows the deraining performance of the traffic rain image database. This traffic frame contains a rain accumulation effect. The JORDER net method retains a minimum level of the rain pattern in the reconstructed output. However, SSDRNET results contain blurred moving objects and backgrounds. When rain streaks are similar to the object movement and orientation, these two methods have some difficulty in removing the rain streaks as well as maintaining background information. The proposed dual-stage derain SRCNN-based attention network provides a better-reconstructed image without any rain pattern. From the various numerical experiments on the real-world data set, it is observed that the proposed dual-stage derain SRCNN net provides superior deraining performance under various rain pattern conditions.

3.3. Ablation experiment. The proposed deraining network consists of different subcomponents such as the derain SRCNN, MRDB, 3SFAM modules. The training of such dual-stage deraining frameworks depends on the individual component performance. Consequently, it is necessary to conduct an ablation study to prove the network performance in deraining applications. We conduct the ablation study by considering the different components of the dual-stage deraining framework. Also, this study provides performance in terms of the overall

Fig. 5. Deraining results of various deraining networks on five synthetic data sets.

PSNR and SSIM values.

Five different types of network architecture are involved in this ablation study:

1. a network without Stage II (derain SRCNN),
2. a network without a modified dense network block,
3. a network with a single-stage derain SRCNN and an MRDB unit,
4. a network without the 3SFAM module,
5. the proposed dual stage deraining framework. The ablation study of the network using a synthetic dataset is presented in Table 3.

The network with a single-stage derain SRCNN provides poor visual performance for different kinds of synthetic data sets. Hence rain patterns are statistically independent and additional CNN blocks to perform deraining tasks. From Table 3 it is observed that the modified dense network plays an important role in achieving better PSNR and SSIM values. The 3SFAM module contributes a minimum performance boost for the proposed method.

3.4. Complexity analysis of the deraining network. The dual-channel RELU (DCReLU) activation function is one of the driving forces to achieve a better reconstruction

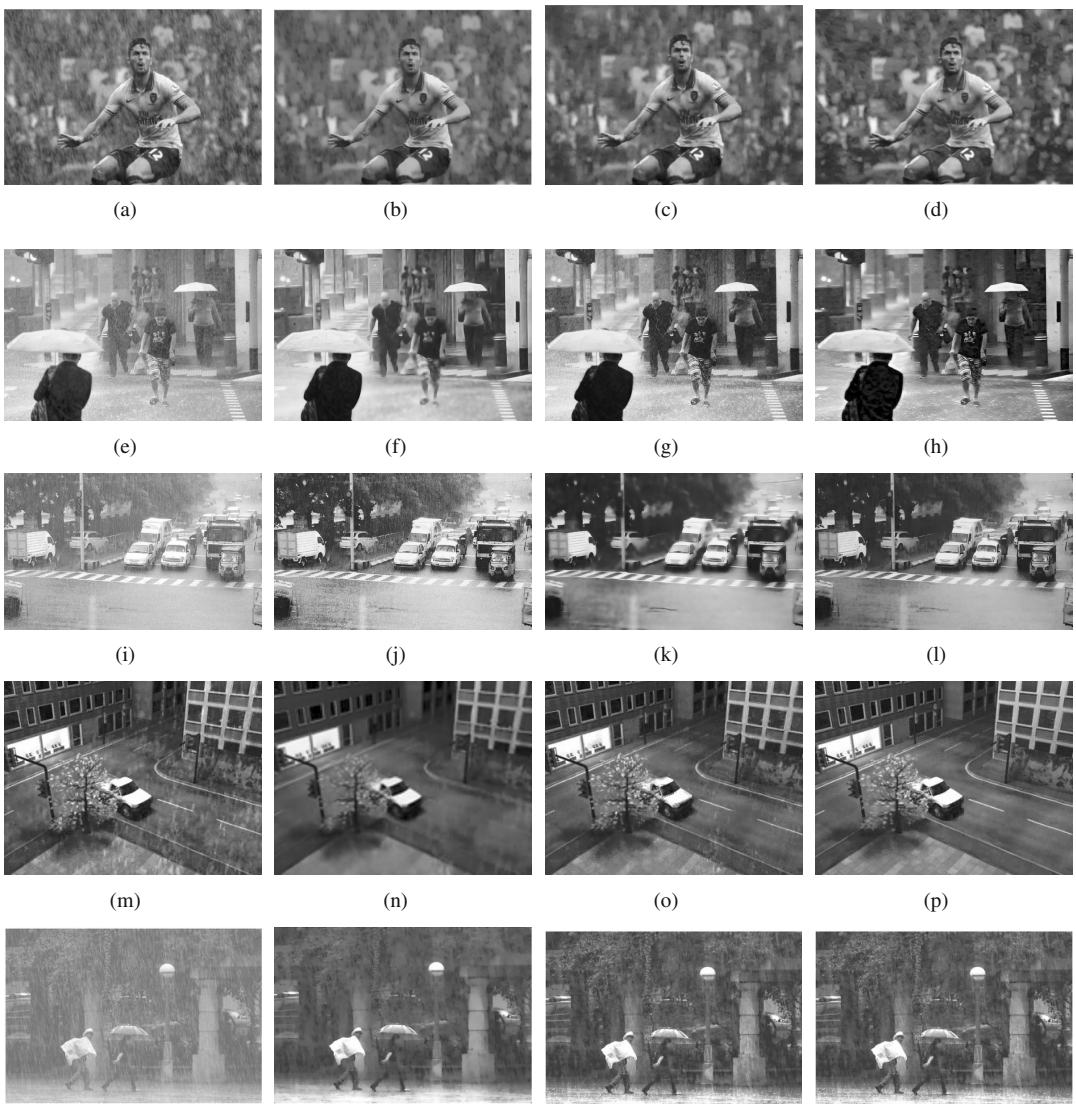

Fig. 6. Deraining results of various deraining networks on real-world rain data sets.

of rainy images and low convergence time. Due to the presence of this activation function, the identification of rain pixels is very fast compared with other activation units such as Tanh or ReLU. During the training stage, the network faces a vanishing gradient problem. This problem regards an unstable behavior of the CNN, causing poor convergence and failure in the weight update process. In the worst case, a deep neural network terminates the training process. With the usage of a proper activation function in the CNN, vanishing gradient issues can be avoided.

In this proposed CNN-based deraining framework, the DCReLU activation function is used to solve the vanishing gradient issues in both the positive and negative phases of the feature map. In both the regions of the feature map, the gradient of the loss function attains a minimum value, rather than zero.

The computational complexity of the proposed method is compared with other rain streak removal deraining networks such as JORDER and SSDRNET. A personal computer with an Intel Core i5 central processing unit (CPU) at 4 GHz and NVIDIA GeForce GTX 2070 with 4 GB memory are the computational environment used in the proposed research study. PyTorch is used to assess the computational complexity of the proposed method. Only a few rain images are considered due to the memory limitation of the hardware platform to test the computation time. The average computation times of synthetic and real-time images are presented in Table 4. From the complexity analysis it is observed that the proposed dual-stage draining framework is faster than the other two draining networks.

Table 3. Deraining results (PSNR/SSIM) with different network architectures.

Network structure	RAIN100L	RAIN100H	DID MDN	DDN net	RESCAN net
Network without Stage II (derain SRCNN)	34.56/0.9253	31.45/0.9045	35.62/0.8756	37.56/0.8953	30.12/0.8652
Network without modified dense network block	31.65/0.9356	24.5/0.8941	29.45/0.8915	32.45/0.9421	26.56/0.8564
Network with single stage derain SRCNN and MRDB unit	36.05/0.9541	30.45/0.9312	34.44/0.8845	36.45/0.9705	28.32/0.9002
Network without 3SFAM module	38.45/0.9654	33.11/0.9425	37.56/0.8992	40.52/0.9854	31.44/0.9125
Proposed dual stage draining framework	40.12/0.9748	35.79/0.9511	40.75/0.9015	42.17/0.9912	34.72/0.9244

Table 4. Computation time.

Data set	Average computation time (sec)		
	JORDER	SSDRNET	Proposed net
RAIN100L	12.50	7.25	3.56
RAIN100H	16.32	4.45	1.45
DID MDN	25.53	14.32	5.65
DDN net	19.45	16.50	10.12
RESCAN net	28.12	21.56	13.56

4. Conclusion

In this paper, a novel dual-stage derain SRCNN model with a residual dense network is developed for single image deraining applications. In this proposed deraining topology the derain SRCNN module is integrated with MRDB and 3SFAM modules to achieve the effective rain pattern removal process. The heavy rain patterns are easily removed due to the presence of the six-stage feature aggregation module and the dual channel ReLU activation unit in this proposed deraining method. The rain component extraction and rain feature refinement process are performed through the cascading stages of MRDB and 3SFAM units. The statistically independent structural rain pattern has been removed through this cascading topology. The effectiveness of the proposed network was also demonstrated through an ablation study wherein the effect of various deraining module changes was studied. Finally, the proposed deraining network topology is trained and tested on a higher-end hardware platform using PyTorch. The extensive quality performance experimental result shows that the proposed deraining network provides higher quality measure values compared with state-of-the-art deraining approaches on five synthetic rain images data set and real-world data sets. In future work, we will further explore the proposed deraining network stages for video deraining applications.

References

Barnum, P.C., Narasimhan, S. and Kanade, T. (2009). Analysis of rain and snow in frequency space, *International Journal of Computer Vision* **86**(2): 256, DOI: 10.1007/s11263-008-0200-2.

Chen, Y. and Wang, W. (2020). Recursive modified dense network for single-image deraining, *Journal of Electronic Imaging* **29**(3): 10–12.

Ding, X., Chen, L., Zheng, X., Huang, Y. and Zeng, D. (2016). Single image rain and snow removal via guided L0 smoothing filter, *Multimedia Tools and Applications* **75**(5): 2697–2712, DOI: 10.1007/s11042-015-2657-7.

Fu, X., Huang, J., Zeng, D., Huang, Y., Ding, X. and Paisley, J. (2017). Removing rain from single images via a deep detail network, *Proceedings of the 30th IEEE Conference on Computer Vision and Pattern Recognition, CVPR 2017, Honolulu, USA*, pp. 1715–1723.

Garg, K. and Nayar, S.K. (2004). Detection and removal of rain from videos, *Proceedings of the 2004 IEEE Computer Society Conference on Computer Vision and Pattern Recognition, CVPR 2004, Washington, USA*, Vol. 1, pp. I–I.

Gu, S., Meng, D., Zuo, W. and Zhang, L. (2017). Joint convolutional analysis and synthesis for sparse representation for single image layer separation, *2017 IEEE International Conference on Computer Vision (ICCV), Venice, Italy*, pp. 1717–1725.

He, K., Zhang, X., Ren, S. and Sun, J. (2016). Deep residual learning for image recognition, *Proceedings of the IEEE*

Computer Society Conference on Computer Vision and Pattern Recognition, Las Vegas, USA, pp. 770–778.

Huang, G., Liu, Z., Van Der Maaten, L. and Weinberger, K.Q. (2017). Densely connected convolutional networks, *Proceedings of the 30th IEEE Conference on Computer Vision and Pattern Recognition, CVPR 2017, Honolulu, USA*, pp. 2261–2269.

Jayaraman, T. and Chinnusamy, G.S. (2020a). Analysis of deep rain streaks removal convolutional neural network-based post-processing techniques in HEVC encoder, *Journal of Circuits, Systems and Computers* **30**(2): 1–21, Paper no. 2150020.

Jayaraman, T. and Chinnusamy, G.S. (2020b). Investigation of filtering of rain streaks affected video sequences under various quantisation parameter in HEVC encoder using an enhanced V-BM4D algorithm, *IET Image Processing* **14**(2): 337–347.

Kang, L., Lin, C. and Fu, Y. (2012). Automatic single-image-based rain streaks removal via image decomposition, *IEEE Transactions on Image Processing* **21**(4): 1742–1755.

Kim, J., Lee, C., Sim, J. and Kim, C. (2013). Single-image deraining using an adaptive nonlocal means filter, *IEEE International Conference on Image Processing, Melbourne, Australia*, pp. 914–917.

Kou, F., Chen, W., Wen, C. and Li, Z. (2015). Gradient domain guided image filtering, *IEEE Transactions on Image Processing* **24**(11): 4528–4539.

Kowal, M., Skobel, M., Gramacki, A. and Korbicz, J. (2021). Breast cancer nuclei segmentation and classification based on a deep learning approach, *International Journal of Applied Mathematics and Computer Science* **31**(1): 85–106, DOI: 10.34768/amcs-2021-0007.

Koziarski, M. and Cyganek, B. (2018). Impact of low resolution on image recognition with deep neural networks: An experimental study, *International Journal of Applied Mathematics and Computer Science* **28**(4): 735–744, DOI: 10.2478/amcs-2018-0056.

Li, P., Tian, J., Tang, Y., Wang, G. and Wu, C. (2020). Model-based deep network for single image deraining, *IEEE Access* **8**(1): 14036–14047.

Li, X., Wu, J., Lin, Z., Liu, H. and Zha, H. (2018). Recurrent squeeze-and-excitation context aggregation net for single image deraining, *Proceedings of the European Conference on Computer Vista (ECCV), Amsterdam, The Netherlands*, pp. 254–269.

Li, Y., Tan, R.T., Guo, X., Lu, J. and Brown, M.S. (2016). Rain streak removal using layer priors, *Proceedings of the IEEE Computer Society Conference on Computer Vision and Pattern Recognition, Las Vegas, USA*, pp. 2736–2744.

Lin, C.Y., Tao, Z., Xu, A.S., Kang, L.W. and Akhyar, F. (2020). Sequential dual attention network for rain streak removal in a single image, *IEEE Transactions on Image Processing* **29**(1): 9250–9265.

Papiez, A., Badie, C. and Polanska, J. (2019). Machine learning techniques combined with dose profiles indicate radiation response biomarkers, *International Journal of Applied Mathematics and Computer Science* **29**(1): 169–178, DOI: 10.2478/amcs-2019-0013.

Paszke, A., Gross, S., Massa, F., Lerer, A., Bradbury, J., Chanan, G., Killeen, T., Lin, Z., Gimelshein, N., Antiga, L., Desmaison, A., Köpf, A., Yang, E., DeVito, Z., Raison, M., Tejani, A., Chilamkurthy, S., Steiner, B., Fang, L., Bai, J. and Chintala, S. (2019). PyTorch: An imperative style, high-performance deep learning library, *arXiv* 1912.01703 (NeurIPS).

Ren, D., Shang, W., Zhu, P., Hu, Q., Meng, D. and Zuo, W. (2020). Single image deraining using bilateral recurrent network, *IEEE Transactions on Image Processing* **29**(1): 6852–6863.

Ren, D., Zuo, W., Hu, Q., Zhu, P. and Meng, D. (2019). Progressive image deraining networks: A better and simpler baseline, *IEEE Conference on Computer Vision and Pattern Recognition, Long Beach, USA* pp. 3937–3946.

Sharma, P.K., Basavaraju, S. and Sur, A. (2021). High-resolution image de-raining using conditional GAN with sub-pixel upscaling, *Multimedia Tools and Applications* **80**(1): 1075–1094, DOI: 10.1007/s11042-020-09642-7.

Sheikh, H.R. and Bovik, A.C. (2006). Image information and visual quality, *IEEE Transactions on Image Processing* **15**(2): 430–444.

Thiyagarajan, J. and Gowri Shankar, C. (2020). Quality improvement and performance analysis of high efficiency video coding under high quantization parameters and rain streaks, *Signal, Image and Video Processing* **14**(2): 387–395, DOI: 10.1007/s11760-019-01565-7.

Wang, C., Zhang, M., Su, Z., Yao, G., Wang, Y., Sun, X. and Luo, X. (2019). From coarse to fine: A stage-wise deraining net, *IEEE Access* **7**(1): 84420–84428.

Wang, M., Chen, L., Liang, Y., Hao, Y., He, H. and Li, C. (2020a). Single image rain removal with reusing original input squeeze-and-excitation network, *IET Image Processing* **14**(8): 1467–1474.

Wang, M., Chen, L., Liang, Y., Huang, H. and Cai, R. (2020b). Deep learning method for rain streaks removal from single image, *Journal of Engineering* **2020**(13): 555–560.

Wang, Y., Gong, D., Yang, J., Shi, Q., van den Hengel, A., Xie, D. and Zeng, B. (2020c). Deep Single Image Deraining via Modeling Haze-like Effect, *IEEE Transactions on Multimedia* **23**(1): 1–1.

Wang, Y., Zhang, D. and Dai, G. (2020d). Classification of high resolution satellite images using improved U-Net, *International Journal of Applied Mathematics and Computer Science* **30**(3): 399–413, DOI: 10.34768/amcs-2020-0030.

Wang, Z. and Bovik, A.C. (2002). A universal image quality index, *IEEE Signal Processing Letters* **9**(3): 81–84.

Wang, Z., Bovik, A.C., Sheikh, H.R. and Simoncelli, E.P. (2004). Image quality assessment: From error visibility to structural similarity, *IEEE Transactions on Image Processing* **13**(4): 600–612.

Wei, W., Meng, D., Zhao, Q., Xu, Z. and Wu, Y. (2018). Semi-supervised transfer learning for image rain removal, *32nd IEEE/CVF Conference on Computer Vision and Pattern Recognition, CVPR 2018, Long Beach, USA*, pp. 3877–3886.

Wu, S. and Zhou, J. (2020). MSFA-Net: A network for single image deraining, *Journal of Physics: Conference Series* **1584**(1), Paper no. 012047.

Yang, W., Tan, R.T., Feng, J., Guo, Z., Yan, S. and Liu, J. (2020). Joint rain detection and removal from a single image with contextualized deep networks, *IEEE Transactions on Pattern Analysis and Machine Intelligence* **42**(6): 1377–1393.

Yang, W., Tan, R.T., Feng, J., Liu, J., Guo, Z. and Yan, S. (2017). Deep joint rain detection and removal from a single image, *2017 IEEE Conference on Computer Vision and Pattern Recognition (CVPR), Honolulu, USA*, pp. 1685–1694.

Zhang, H. and Patel, V.M. (2018). Density-aware single image de-raining using a multi-stream dense network, *Proceedings of the IEEE Computer Society Conference on Computer Vision and Pattern Recognition, San Juan, USA*, pp. 695–704.

Zhang, L., Zhang, L., Mou, X. and Zhang, D. (2011). FSIM: A feature similarity index for image quality assessment, *IEEE Transactions on Image Processing* **20**(8): 2378–2386.

Zhang, Y., Tian, Y., Kong, Y., Zhong, B. and Fu, Y. (2018). Residual dense network for image super-resolution, *Proceedings of the IEEE Computer Society Conference on Computer Vision and Pattern Recognition, Salt Lake City, USA,* pp. 2472–2481.

Thiyagarajan Jayaraman holds a PhD degree from Anna University, along with a BE degree in electronics and communication engineering from the Sona College of Technology. He also holds an ME degree in power electronics and drives from the Kumarguru College of Technology, Coimbatore. From 2008 to 2011 he worked as an assistant professor in the Department of Electronics and Communication Engineering, Sengunthar College of Engineering, Tiruchengode, Tamil Nadu, India. From 2011 to 2021 he worked as an assistant professor in the Electronics Engineering Department of the KSR College of Engineering, Namakkal. Currently he is an assistant professor with the Sona College of Technology, Salem. His scientific interests include image processing, video processing, computer vision and machine learning.

Gowri Shankar Chinnusamy received his BE degree in electrical and electronics engineering from Periyar University in 2003 and his ME degree in applied electronics from Anna University, Chennai, in 2005. He completed his PhD in medical image processing at Anna University in 2013. In 2005–2010, he worked as an assistant professor in the Department of Electrical and Electronics Engineering, Velalar College of Engineering and Technology, Erode, Tamil Nadu, India. Currently, he is a professor in the Department of Electrical and Electronics Engineering, KSR College of Engineering, Tiruchengode, Tamil Nadu, India. His research interests are in multirate signal processing, computer vision, medical image processing and pattern recognition.

Received: 9 July 2021
Revised: 3 December 2021
Accepted: 26 January 2022